

Dalton Transactions

Accepted Manuscript



This is an *Accepted Manuscript*, which has been through the Royal Society of Chemistry peer review process and has been accepted for publication.

Accepted Manuscripts are published online shortly after acceptance, before technical editing, formatting and proof reading. Using this free service, authors can make their results available to the community, in citable form, before we publish the edited article. We will replace this *Accepted Manuscript* with the edited and formatted *Advance Article* as soon as it is available.

You can find more information about *Accepted Manuscripts* in the [Information for Authors](#).

Please note that technical editing may introduce minor changes to the text and/or graphics, which may alter content. The journal's standard [Terms & Conditions](#) and the [Ethical guidelines](#) still apply. In no event shall the Royal Society of Chemistry be held responsible for any errors or omissions in this *Accepted Manuscript* or any consequences arising from the use of any information it contains.



Journal Name

ARTICLE

Kinetics and Mechanisms of Reactions between H₂O₂ and Copper and Copper Oxides

Received 00th January 20xx,
Accepted 00th January 20xx

DOI: 10.1039/x0xx00000x

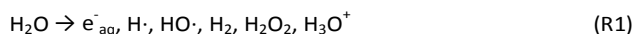
www.rsc.org/

Åsa Björkbacka,^a Miao Yang,^a Claudia Gasparri,^{a†} Christofer Leygraf^b and Mats Jonsson^a

One of the main challenges for the nuclear power industry today is the disposal of spent nuclear fuel. One of the most developed methods for long term storage is the Swedish KBS-3 concept where the spent fuel will be sealed inside copper canisters and placed 500 meters down in the bedrock. Gamma radiation will penetrate the canisters and be absorbed by groundwater thereby creating oxidative radiolysis products such as hydrogen peroxide (H₂O₂) and hydroxyl radicals (HO·). Both H₂O₂ and HO· are able to initiate corrosion of the copper canisters. In this work the kinetics and mechanism of reactions between the stable radiolysis product, H₂O₂, and copper and copper oxides were studied. Also the dissolution of copper into solution after reaction with H₂O₂ was monitored by ICP-OES. The experiments show that both H₂O₂ and HO· are present in the systems with copper and copper oxides. Nevertheless, these species do not appear to influence the dissolution of copper to the same extent as observed in recent studies in irradiated systems. This strongly suggest that aqueous radiolysis can only account for a very minor part of the observed radiation induced corrosion of copper.

Introduction

Radioactive waste in the form of spent nuclear fuel constitutes one of the inevitable environmental challenges of nuclear power. The spent, or used, nuclear fuel can also be seen as a resource for the manufacturing of new fuel via reprocessing. However, several countries have decided to use a once-through fuel cycle with final disposal of the spent fuel. One of the most developed methods for long-term geological storage of high level spent nuclear fuel is the Swedish multi barrier KBS-3 concept. In this concept, the spent fuel elements will be placed inside sealed copper-cast iron canisters, embedded in bentonite clay and deposited 500 meters down in the bedrock.¹ The purpose of the outer copper layer is to prevent corrosion in the reducing environment prevailing at this depth in granitic bedrock. The canisters will be surrounded by bentonite clay acting as a mechanical buffer and providing diffusion resistance for the transport of corrosive agents to the canister surface, as well as radionuclides from the canister in case of canister failure. Due to the high specific activity of the spent nuclear fuel, neutron and gamma radiation will penetrate the cast iron and the copper and be absorbed by the surrounding clay. The clay will contain groundwater that will undergo radiolysis upon absorption of the ionizing radiation. Radiolysis of water produces oxidizing and reducing species in accordance with Reaction 1 (R1).²



Two of the radiolysis products, hydrogen peroxide (H₂O₂) and the hydroxyl radical (HO·), are thermodynamically capable of corroding copper as they have higher standard reduction potentials (E⁰) than copper.³⁻⁵ Nevertheless, previous studies on radiation induced corrosion of copper under anoxic conditions have presented conflicting conclusions.⁶⁻⁹ However, the total absorbed doses employed in these studies differ significantly.

Recent studies, employing absorbed gamma doses close to the ones expected at the outer copper surface in a deep repository during the first 100 years, have shown that copper, in anoxic aqueous solution corrodes significantly.^{6, 7} The corrosion appears both as an oxide layer and as local corrosion features. The latter are commonly circular in shape with copper oxide in the center surrounded by a circle of bare metal surface. The main corrosion product formed on the copper surface is copper(I)oxide (Cu₂O) together with a small fraction of copper(II)oxide (CuO).^{6, 7} Copper release into aqueous solution was also monitored (using ICP-OES) as a function of absorbed dose. The measured concentrations of released copper increase with the absorbed dose to values that are significantly higher than the solubility of the oxides formed. Furthermore, the magnitude of the corrosion vastly exceeds what could be expected from homogeneous aqueous radiolysis. Admittedly, neither the local corrosion features nor the extremely high concentrations of copper in solution could be satisfactorily accounted for.

To further investigate this system we decided to undertake a study of the kinetics and mechanism of reactions between the

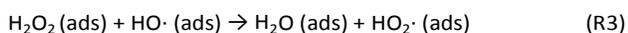
^a Division of Applied Physical Chemistry, KTH Royal Institute of Technology, School of Chemical Science and Engineering, SE-100 44 Stockholm, Sweden.

^b Division of Surface and Corrosion Science, KTH Royal Institute of Technology, School of Chemical Science and Engineering, SE-100 44 Stockholm, Sweden.

[†] Current address: Centre for Nuclear Engineering, Imperial College London, Prince Consort Road, London SW7 2AZ, UK

stable aqueous radiolysis product H_2O_2 and copper and copper oxides.

H_2O_2 has been identified as the most important oxidant in radiation induced dissolution of UO_2 -based nuclear fuel and for this reason it has been studied quite extensively in recent years.¹⁰⁻¹⁴ H_2O_2 reacts with some metal oxides via both electron-transfer¹⁵ and catalytic decomposition.¹⁶ The former reaction leads to corrosion while the latter consumes H_2O_2 leaving the oxide in its original oxidation state. Cu(II) can also oxidize H_2O_2 . However, the impact of this reaction is negligible given the low concentration of Cu(II) ,¹⁷ and the low pseudo-order rate constant for the reaction, the order of 10^{-6} s^{-1} ,¹⁸⁻²⁰ (at pH 6 and 10 μM of Cu(II)). A plausible mechanism of the catalytic decomposition is summarized in Reaction 2-4 (R2-R4).^{10, 14, 16}



Here, (ads) represents a surface adsorbed state. Adsorption of the hydroxyl radical is a thermodynamic prerequisite for this reaction to occur. It is interesting to note that in solution, it has been shown that complexes of metal ions such as Al(III) and Co(II) catalyze production of $\text{HO}\cdot$ from H_2O_2 .^{21, 22} The formation of O_2 (R4) has been confirmed in several studies. The initial formation of hydroxyl radicals was confirmed quite recently using tris(hydroxymethyl)aminomethane (TRIS) as a probe.¹³ Upon hydrogen abstraction, TRIS produces formaldehyde that can be readily detected. However, TRIS contains an amino group that can sometimes interact with the metal of interest and thereby influence the solubility of a metal oxide. For copper this is a significant problem since copper ions display a high affinity for amino groups.²³ Hence, using TRIS as a probe for hydroxyl radical formation on copper or copper oxides is not possible since the detection of formaldehyde is based on spectrophotometry. Copper-amino complexes may interfere with these measurements. However, methanol (CH_3OH) can also be used as a probe for the hydroxyl radical.²⁴⁻²⁶ The main product from the reaction between CH_3OH and $\text{HO}\cdot$ is the hydroxymethyl radical ($\cdot\text{CH}_2\text{OH}$) which accounts for approximately 93% of the products.²⁷ In deoxygenated solution $\cdot\text{CH}_2\text{OH}$ reacts further, to form mainly ethylene glycol (CH_2OH)₂ and secondly CH_2O , via disproportionation.^{28, 29} The reaction between CH_3OH and $\text{HO}\cdot$ has recently been studied experimentally on the basis of gamma irradiation of anoxic CH_3OH -solution where CH_2O was detected. The yield was found to be 14%.²⁶ $\cdot\text{CH}_2\text{OH}$ can also react with H_2O_2 and aqueous Cu(II) , forming CH_2O as well.^{30, 31} It is also interesting to note that the methyl radical ($\cdot\text{CH}_3$) can react with metallic copper (Cu^0) via a surface reaction, to form CH_3OH .³² This might suggest that $\cdot\text{CH}_2\text{OH}$ (from the reaction between $\text{HO}\cdot$ and CH_3OH) is also able to react with Cu^0 and further generate CH_2O . As there are several possible reaction

pathways for $\cdot\text{CH}_2\text{OH}$ the yield of CH_2OH obtained in this study must be considered a relative measurement of $\text{HO}\cdot$.

Although CH_3OH has a low CH_2O yield in the absence of O_2 , it does not display the disadvantage of forming light absorbing complexes with copper ions. Also the concentrations of dissolved Cu(I) and Cu(II) are much lower than the concentrations of H_2O_2 and CH_3OH that are used in this study. For these reasons, we chose to use CH_3OH as a probe for the catalytic decomposition of H_2O_2 on copper and copper oxides. In addition to powder suspensions of Cu , Cu_2O and CuO , we also studied $10 \times 10 \times 10 \text{ mm}$ cubes of copper.

In order to further understand the interfacial processes occurring during the reaction between H_2O_2 and copper, the consumption of H_2O_2 and the production of CH_2O from the reaction between CH_3OH and $\text{HO}\cdot$ were studied spectrophotometrically as a function of time. The release of copper into aqueous solution was monitored using ICP-OES.

The previously observed corrosion phenomena are discussed in view of the results of the present study.

Results and discussion

Kinetics of H_2O_2 consumption

In Figure 1, the concentration of H_2O_2 as a function of reaction time is presented for Cu -, Cu_2O -, and CuO -powder respectively.

The concentrations of H_2O_2 were measured over time, in the presence of varying amounts of copper and copper oxides. The initial experimental conditions were 50 ml aqueous solution of 0.5 mM H_2O_2 with continuous nitrogen purging at ambient temperature. The pH for all solutions before, during and after the reactions was approximately 6.

The results displayed in Figure 1 clearly show that the rate of H_2O_2 consumption increases with increasing amount of powder present for all three materials. However, to be able to compare the H_2O_2 reactivity of the three materials we should determine the second order rate constants for the reactions. This is obtained as the slope of a plot of the first order rate constants as a function of the solid-surface-area-to-solution-volume ratios. Admittedly, the reaction order of the reactions presented in Figure 1 is not always one throughout the entire reaction. Using the initial part of the plots, this problem is to some extent circumvented. In Figure 2, the first order rate constants are plotted against the solid surface-area-to-solution-volume ratio for the three powders.

From Figure 3 it can be seen that for solid surface-area-to-solution-volume ratios of Cu_2O , below 400 m^{-1} , the consumption of H_2O_2 is independent of the surface area of the oxide. This can probably be attributed to the reaction between H_2O_2 and dissolved Cu(I) in the Fenton reaction³³ (the aqueous solubility at pH 6 is approximately $1 \mu\text{M}$ from Cu_2O and $10 \mu\text{M}$ from CuO ¹⁷) or the reaction between H_2O_2 with Cu(I) and Cu(II) in the Haber-Weiss reaction. In this reaction, it is the reduction of Cu(II) that is the rate limiting step. It is also suggested that H_2O_2 can oxidize Cu(I) directly to Cu(III) .^{31, 34, 35} Cu(III) could

also react further with CH_3OH resulting in $\cdot\text{CH}_2\text{OH}$.³⁶ This reaction is however slow under the present neutral conditions.³⁷ The rates of these reactions are simply governed by the solubility of Cu(I) .

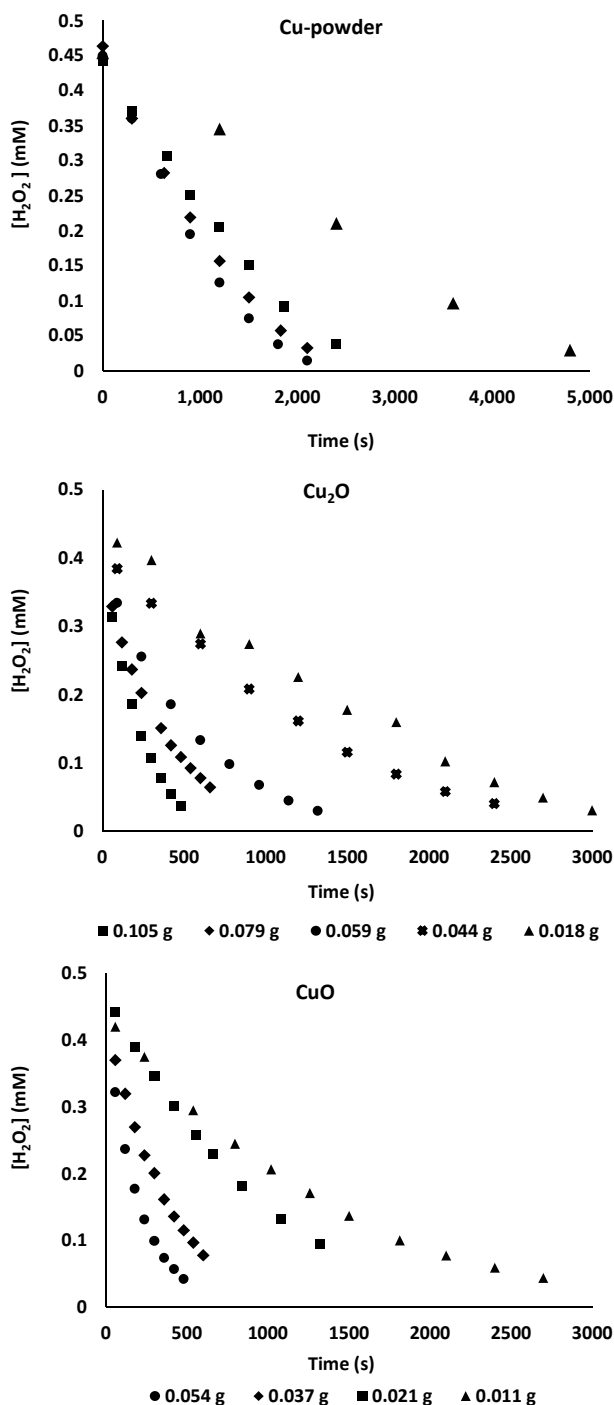


Figure 1. The concentration of H_2O_2 as a function of time in the presence of Cu-, Cu_2O - and CuO-powder is shown.

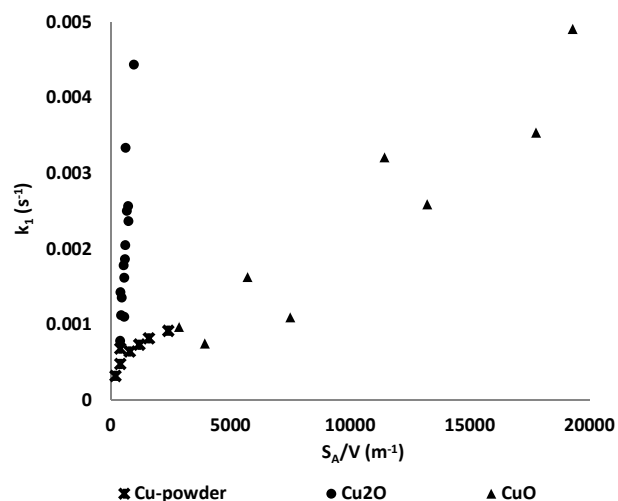


Figure 2. First order rate constants, $k_1 \text{ (s}^{-1}\text{)}$, for H_2O_2 (50 ml 0.5 mM H_2O_2) consumption as a function of solid surface-area-to-solution-volume ratio for Cu-, Cu_2O - and CuO-powder.

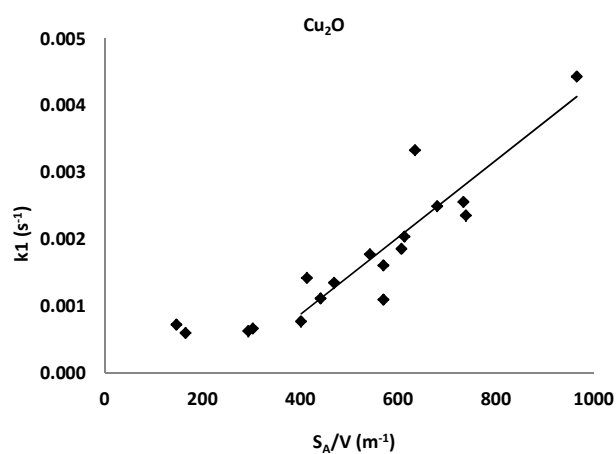


Figure 3. An enlargement of the plot of first order rate constants, $k_1 \text{ (s}^{-1}\text{)}$, for H_2O_2 consumption on Cu_2O as a function of solid surface-area-to-solution-volume ratios, presented in Figure 2.

For solid surface-area-to-solution-volume ratios above 400 m^{-1} , the rate of H_2O_2 consumption increases with increasing amount of Cu_2O . Hence, the surface reactions are becoming competitive with the solution reaction under these conditions. The second order rate constant for consumption of H_2O_2 on Cu_2O is obtained from solid surface-area-to-solution-volume ratios above 400 m^{-1} . These solution reactions are not observed for the reactions of CuO - and Cu -powder with H_2O_2 . In the mechanistic study presented below, the surface-area-to-solution-volumes for all three powders are much higher than 400 m^{-1} and therefore the contribution of $\text{HO}\cdot$ from homogeneous solution reactions is negligible.

When measuring dissolution of copper into solution after the reaction of 1.5 g of Cu -powder and 50 ml of 0.5 mM of H_2O_2 the concentration was approximately $1 \mu\text{M}$, which is in the range of solubility for Cu_2O and CuO .¹⁷

In Table 1 the corresponding rate constants and powder characteristics are presented. The particle sizes of the three different powders are estimated from SEM examinations. Judging from the second order rate constants presented in Table 1 Cu_2O displays the highest reactivity towards H_2O_2 while Cu and CuO are 20 times less reactive. However, it is important to keep in mind that the *diffusion limited rate constant* for heterogeneous reactions depends on the particle size. Smaller particles have a higher diffusion limited rate constant than larger particles. To compare surface reactivity we should thus compare the estimated size normalized relative rate constants, also presented in Table 1.³⁸ According to the theory presented in Ref 23, the diffusion limited rate constant for a reaction between solute reactants and reactants at a particle surface is inversely proportional to the particle size. Hence, by multiplying the second order rate constants determined above with each particle size used in the experiments and then compare them with each other, we obtain size normalized relative rate constants that can be used when comparing the reactivity of different materials.

From the estimated size normalized relative rate constant we can conclude that CuO is less reactive than Cu_2O - and Cu -powders. This can largely be attributed to the fact that H_2O_2 can only undergo catalytic decomposition on CuO while electron-transfer is an additional possibility for the other two materials. Cu_2O still appears to be the most reactive material.

Table 1. Second-order rate constants, k_2 ($\text{m}\cdot\text{s}^{-1}$) and estimated size normalized relative rate constants for the consumption of H_2O_2 on Cu -, Cu_2O - and CuO -powder. Also the B.E.T.-surface areas ($\text{m}^2\cdot\text{g}^{-1}$) and estimated particle sizes (μm) are given.

Material	Estimated particle size (μm)	B.E.T.-surface area ($\text{m}^2\cdot\text{g}^{-1}$)	2 nd order rate constant, k_2 ($\text{m}\cdot\text{s}^{-1}$)	Estimated size normalized relative rate constant (Arb.)
Cu-powder	10-100	0.1	$2.2\pm 0.6\cdot 10^{-7}$	100-1000
Cu_2O	0.5-15	0.5	$5.8\pm 0.8\cdot 10^{-6}$	130-4000
CuO	0.1-10	17.9	$2.2\pm 0.3\cdot 10^{-7}$	1-100

Mechanism

With the exception of CuO (where copper is in its highest oxidation state), H_2O_2 can react with the powders in two ways: either by oxidation of the powder or by catalytic decomposition of H_2O_2 on the oxide surface.

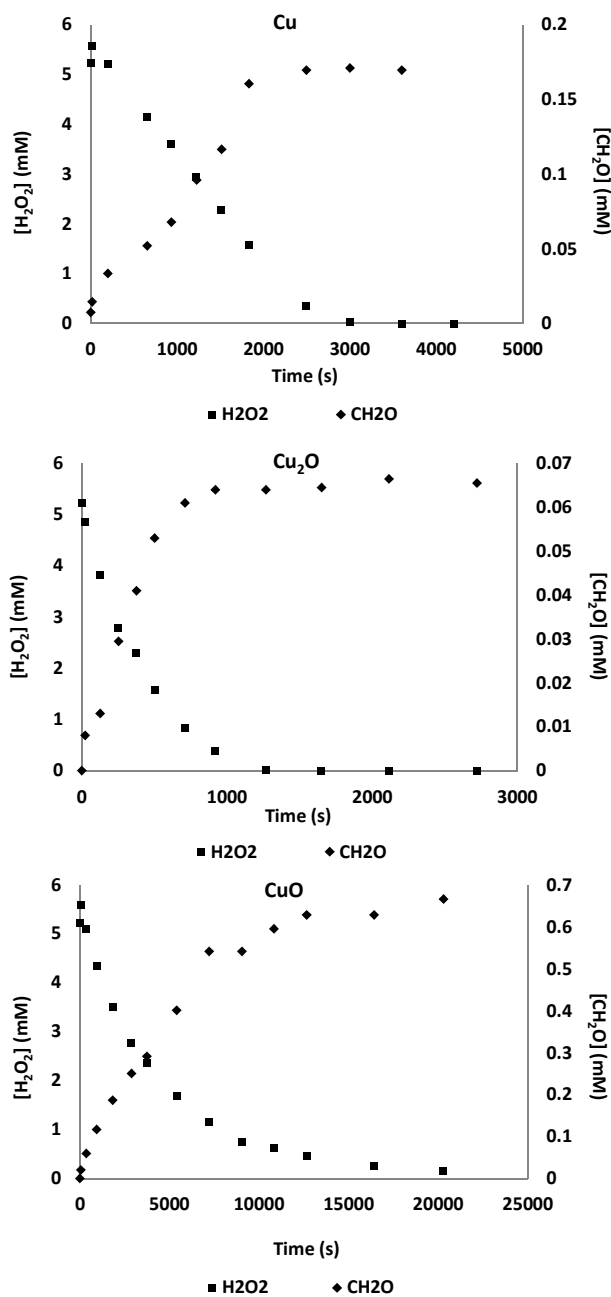


Figure 4. The consumption of H_2O_2 and the production of CH_2O as a function of reaction time for Cu -, Cu_2O - and CuO -powder.

The relative impact of catalytic decomposition of H_2O_2 was monitored using CH_3OH as a scavenger for the hydroxyl radical formed in the process and quantifying the amount of formaldehyde produced in the process. The yield of formaldehyde from CH_3OH and $\cdot\text{OH}$ under homogenous anoxic conditions is only 14 %.²⁶ Therefore the concentrations of formaldehyde detected in this study are expected to be quite low.

In Figure 4, the formaldehyde production and the H_2O_2 consumption are plotted against reaction time for the three materials. Here, the solid surface-area-to-solution-volume ratios are the same in all three cases ($4600 \pm 200 \text{ m}^{-1}$).

As can clearly be seen, the yield of formaldehyde is highest for CuO . This is not surprising since catalytic decomposition is the only possible reaction pathway for consuming H_2O_2 in this system. For Cu and Cu_2O , the formaldehyde yield is lower which is attributed to the competition between surface oxidation and catalytic decomposition.

Copper cubes

Cu -cubes were used in previous experiments on radiation induced dissolution of copper. In this work we also used Cu -cubes to elucidate the H_2O_2 reactivity and the mechanism of the reaction. In addition to monitoring the H_2O_2 consumption and formaldehyde production, we also measured the concentration of copper in the reaction solutions using ICP-OES. When measuring release of copper into solution after the reaction of a Cu -cube and 50 ml of 0.5 mM of H_2O_2 the concentration was approximately 2 μM , which is in the range of the solubility of Cu_2O and CuO . This contradicts the significantly higher copper concentrations observed for irradiated copper cubes.⁷ Consequently, radiolytically produced H_2O_2 cannot account for the observed copper release upon irradiation. In Figure 5, the H_2O_2 and formaldehyde concentrations are plotted as a function of reaction time for polished and pre-oxidized Cu -cubes.

It is important to note that the solid-surface-area-to-solution-volume ratio is very small in these experiments, only 6 m^{-1} . At this solid-surface-area-to-solution-volume ratio ($\ll 400 \text{ m}^{-1}$) the consumption of H_2O_2 is mainly governed by the solution phase Fenton- or Haber-Weiss-chemistry. In addition, this means that the monitored H_2O_2 consumption and CH_2O production in Figure 5 can only to a small extent be attributed to surface reactivity. In Figure 5 it can also be seen that the H_2O_2 consumption is slightly faster for the pre-oxidized Cu -cube. This might be due to the immediate dissolution of copper ions, from the already formed oxide layer. Also the formaldehyde formation displays a difference between the two Cu -cubes; the yield is significantly higher for the pre-oxidized one. This too is attributed to the presence of oxide from the very beginning.

When comparing the results of the present study to results of previous studies on radiation induced corrosion of copper there is, as stated above, an obvious difference in the amount of copper released to the solution⁷. In the present study we obtain copper concentrations in solution that are in full

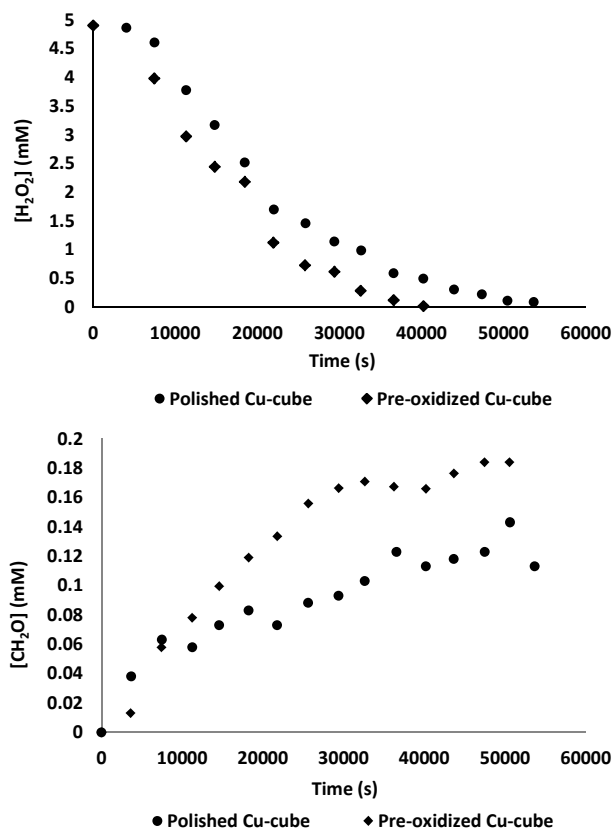


Figure 5. The consumption of H_2O_2 and the production of CH_2O from the reactions between H_2O_2 and Cu -cubes.

agreement with the solubilities reported for the two oxides that are formed. The mechanistic studies using CH_3OH as a scavenger for hydroxyl radicals clearly show that hydroxyl radicals are formed in the systems studied in this work. Hence, both H_2O_2 and hydroxyl radicals are present also in the non-irradiated systems that have only been exposed to H_2O_2 . Nevertheless, these species do not appear to influence the copper release to the same extent as observed in the irradiated system. Again, this strongly indicates that aqueous radiolysis can only account for a very minor part of the observed radiation induced corrosion of copper.

Experimental

Reagents

Cu -powder (CAS [7440-50-8], spherical, -100/+325 mesh, 99.9 %, Alfa Aesar), copper(I)oxide (Cu_2O), (CAS [1317-39-1], powder, anhydrous, 99.9 %, Sigma-Aldrich), copper(II)oxide (CuO): (CAS [1317-38-0], powder, 99.99 %, Aldrich) were used without further purification. Nitrogen adsorption-desorption isotherms were recorded at liquid nitrogen temperature (77K) for all powders using a Micromeritics ASAP2020 volumetric adsorption analyser. The samples were treated under near-vacuum conditions ($< 10^{-5}$ Torr) at a temperature of 300°C for 10 h before the measurements. The specific surface areas of

the materials were calculated from the recorded data, of adsorption and desorption of N_2 gas onto the powders, employing to the B.E.T. isotherm.^{39, 40} The range of relative pressures (p/p_0) were 0.05 - 0.15, where p_0 is the saturation pressure of the gas and p is the equilibrium pressure of the gas. The equilibration time was 10 s. 5 to 6 isotherms were used for each B.E.T. surface area plot and the linear regression coefficient was at least 0.999.

The total pore volume was calculated at a relative pressure of 0.99. The B.E.T surface areas of the three different powders were: Cu-powder ($0.1 \text{ m}^2\text{g}^{-1}$); Cu_2O ($0.5 \text{ m}^2\text{g}^{-1}$); CuO ($17.9 \text{ m}^2\text{g}^{-1}$).

All powder samples were weighted on a Mettler Toledo AT261 Delta Range Microbalance and all solutions were prepared using water from a Millipore Milli-Q system ($18.2 \text{ M}\Omega\text{cm}^{-1}$). Cu-cubes, originating from a SKB copper canister wall, (99.992% Cu, major impurities are Ag and P) of the sizes $10\times 10\times 10 \text{ mm}$ were polished on all sides with SiC abrasive papers of 1200 grit. One side was further polished with $3 \mu\text{m}$ polycrystalline diamond paste (Struers). All polishing steps were made in 99.5% ethanol. After polishing, the Cu-cubes were placed in 99.5 % ethanol in an ultra-sonic bath for five minutes and then dried under N_2 (AGA Gas AB, purity of 99.996%) in a glovebox. Both freshly polished Cu-cubes and oxidized Cu-cubes were used in this study. The latter were oxidized in 2.5 mM of H_2O_2 for 24 hours. When Cu-cubes are oxidized under these conditions an oxide layer is formed that mainly consists of Cu_2O with a small contribution of CuO .⁷ Still there is not a homogeneous oxide layer covering the pre-oxidized Cu-cube but a heterogeneous layer where there are surface areas covered with oxide and surface areas of bare copper metal. Also local corrosion features can be seen. In Figure 6 SEM images of the starting materials for the reactions between copper and H_2O_2 can be seen.

An inert atmosphere was kept using a constant flux of N_2 gas (AGA Gas AB, purity of 99.996 %) and all experiments were performed at ambient temperature. The aqueous particle suspensions were stirred using a magnetic stirrer at 750 rpm and purged with N_2 at least 30 minutes prior to the experiments.

Kinetic study

The H_2O_2 -solutions were prepared from a 30 % standard solution (CAS [7722-84-1], Merck). Determination of the concentration of H_2O_2 as a function of time was made using the Ghormley triiodide method. In this method, I^- is oxidized to I_3^- by H_2O_2 . The absorbance of the product I_3^- was measured spectrophotometrically at a wavelength of 355 nm. There is a linear correlation between the absorbance of I_3^- and the H_2O_2 concentration.¹⁰ An extracted sample volume of 0.2 ml was filtered through a Gema Medical Cellulose Acetate syringe filter $0.2 \mu\text{m}/13 \text{ mm}$ and further used for the measurement of the H_2O_2 concentration. The solutions were covered with aluminium foil to avoid production of H_2O_2 from water and UV-light. The pH of the oxide suspensions was approximately 6 before, during and after the reactions. The pH was measured

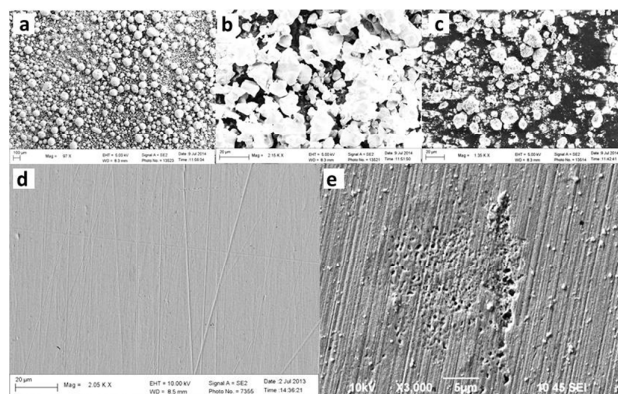


Figure 6. SEM images of the starting materials are shown; (a) Cu-powder, (b) Cu_2O , (c) CuO , (d) a freshly polished Cu-cube and (e) a pre-oxidized Cu-cube.

using a 713 pH Meter from Metrohm. The initial experimental conditions for the reactions between H_2O_2 and powders were 50 ml 0.5 mM of H_2O_2 and the amounts of powders were varied between 0.007 and 1.5 g. Two sets of experimental conditions were used for the reactions between H_2O_2 and Cu-cubes. Initial experimental conditions were 50 ml 0.5 mM of H_2O_2 or 100 mM of CH_3OH in 100 ml 5 mM of H_2O_2 . No change in absorbance was spectrophotometrically detected for possible background reactions between copper and $\text{H}_2\text{O}/\text{CH}_3\text{OH}/\text{CH}_2\text{O}$.

Mechanistic study

The reaction between CH_3OH (HPLC grade CH_3OH , (CAS [67-56-1]), Aldrich, 99,9 %) and $\text{HO}\cdot$ producing CH_2O ²⁶ was monitored using a modified version of the Hantzsch reaction to quantify the amount of CH_2O ⁴¹. The CH_2O reacts further with Acetoacetanilide AAA (CAS[102-01-2], Alfa Aesar, 98%) and Ammonium acetate (CAS[631-61-8], 98 %, Lancaster) to form a dihydropyridine derivative with maximum absorbance wavelength at 368 nm. An extracted sample volume of 1.5 ml was filtered through a Gema Medical Cellulose Acetate syringe filter $0.2 \mu\text{m}/13 \text{ mm}$ and further used for the measurement of the CH_2O concentration. The solutions were covered with aluminium foil to avoid production of H_2O_2 from water and UV-light. The initial experimental conditions for the reactions between H_2O_2 and powders were 100 mM of CH_3OH in 50 ml 5 mM of H_2O_2 and the amounts of powders were varied between 0.0125 and 3 g. The initial experimental conditions for the reactions between H_2O_2 and Cu-cubes were 100 mM of CH_3OH in 100 ml 5 mM of H_2O_2 . No change in absorbance was spectrophotometrically detected for possible background reactions between copper and $\text{H}_2\text{O}/\text{CH}_3\text{OH}/\text{CH}_2\text{O}$.

Instrumentation

UV/vis spectra were collected using a WPA Biowave II UV/vis spectrophotometer. Trace elemental analysis was performed on solutions from Cu-powder and Cu-cubes using inductively coupled plasma atomic emission spectroscopy (Thermo Scientific iCAP 6000 series ICP spectrometer (ICP-OES)). The

analyses for copper were performed at wavelengths of 219.9 and 217.8 nm using ICP single element standard Cu from Merck. Before the measurements all solutions were filtrated through Gema Medical Cellulose Acetate syringe filters 0.2 $\mu\text{m}/13$ mm. Surface examinations using a FEG-SEM Zeiss Sigma VP with a Gemini field emission column scanning electron microscope and a Jeol JSM-6490LV scanning electron microscope with a Jeol EX-230 energy dispersive X-ray spectrometer were performed for powders and Cu-cubes.

Conclusions

- When H_2O_2 is consumed in reactions with Cu-, Cu_2O - and CuO-powder, surface bound $\cdot\text{OH}$ from catalytic decomposition is formed.
- The consumption of H_2O_2 , in the presence of Cu_2O at solid surface-area-to-solution-volume ratios below 400 m^{-1} , occurs primarily through the Fenton reaction in solution.
- Cu_2O is most efficient in consuming H_2O_2 while CuO is most efficient in forming $\cdot\text{OH}$.
- Consumption of H_2O_2 on polished copper surfaces is slower than on oxidized copper surfaces.
- The release of copper upon exposure to H_2O_2 solutions (2 μM) is in agreement of the solubility of Cu_2O and CuO in aqueous solution at pH 6 and 25 °C (1 and 10 μM respectively).

Acknowledgements

The Swedish Nuclear Fuel and Waste Management Co., SKB AB is gratefully acknowledged for financial support. Madeleine Ekström is acknowledged for performing surface examinations.

Notes and references

- 1 B. Rosborg and L. Werme, *Journal of Nuclear Materials*, 2008, **379**, 142-153.
- 2 J. W. T. Spinks and R. J. Woods, *An introduction to radiation chemistry*, Wiley, 1990.
- 3 R. R. Conry, in *Encyclopedia of Inorganic Chemistry*, ed. R. B. King, Wiley, New York, Second edn., 2005, pp. 940-958.
- 4 W. H. Koppenol and J. F. Liebman, *Journal of Physical Chemistry*, 1984, **88**, 99-101.
- 5 F. A. Cotton and G. Wilkinson, *Advanced inorganic chemistry*, Wiley Interscience, New York, 3rd edn., 1972.
- 6 Å. Björkbacka, S. Hosseinpour, C. Leygraf and M. Jonsson, *Electrochemical and Solid-State Letters*, 2012, **15**, C5-C7.
- 7 Å. Björkbacka, S. Hosseinpour, M. Johnson, C. Leygraf and M. Jonsson, *Radiation Physics and Chemistry*, 2013, **92**, 80-86.

- 8 F. King, C. D. Litke and S. R. Ryan, *Corrosion Science*, 1992, **33**, 1979-1995.
- 9 J. P. Simpson, *Experiments on container materials for Swiss high-level waste disposal projects. Part II*, Report Nagra Technical Report 84-01, National Cooperative for the Disposal of Radioactive Waste, Wettingen, 1984.
- 10 C. M. Lousada, M. Trummer and M. Jonsson, *Journal of Nuclear Materials*, 2013, **434**, 434-439.
- 11 E. Ekeröth, O. Roth and M. Jonsson, *Journal of Nuclear Materials*, 2006, **355**, 38-46.
- 12 O. Roth and M. Jonsson, *cent.eur.j.chem.*, 2008, **6**, 1-14.
- 13 C. M. Lousada and M. Jonsson, *Journal of Physical Chemistry C*, 2010, **114**, 11202-11208.
- 14 C. M. Lousada, A. J. Johansson, T. Brinck and M. Jonsson, *The Journal of Physical Chemistry C*, 2012, **116**, 9533-9543.
- 15 V. M. Goldschmidt, *Naturwissenschaften*, 1932, **20**, 947-948.
- 16 A. Hiroki and J. A. LaVerne, *Journal of Physical Chemistry B*, 2005, **109**, 3364-3370.
- 17 D. A. Palmer, P. Benezeth and J. M. Simonson, in *Water, steam and aqueous solutions for electric power: Advances in science and technology. Proc. 14th Int. Conf. on the Properties of Water and Steam, 29 August–3 September 2003*, eds. M. Nakahara, N. Matubayasi, M. Ueno, K. Yasuoka and K. Watanabe, Kyoto, Japan, 2004 (2005), pp. 491–496.
- 18 H.-J. Lee, H. Lee and C. Lee, *Chemical Engineering Journal*, 2014, **245**, 258-264.
- 19 V. K. Sharma and F. J. Millero, *Environmental Science & Technology*, 1988, **22**, 768-771.
- 20 J. F. Perez-Benito, *Journal of Inorganic Biochemistry*, 2004, **98**, 430-438.
- 21 A. Burg, I. Shusterman, H. Kornweitz and D. Meyerstein, *Dalton Transactions*, 2014, **43**, 9111-9115.
- 22 M. L. Kuznetsov, Y. N. Kozlov, D. Mandelli, A. J. L. Pombeiro and G. B. Shul'pin, *Inorganic Chemistry*, 2011, **50**, 3996-4005.
- 23 H. W. Richardson, *Handbook of Copper Compounds and Applications*, Taylor & Francis, 1997.
- 24 A. Monod, A. Chebbi, R. Durand-Jolibois and P. Carlier, *Atmospheric Environment*, 2000, **34**, 5283-5294.
- 25 H. A. Headlam and M. J. Davies, *Free Radical Biology and Medicine*, 2002, **32**, 1171-1184.
- 26 M. Yang and M. Jonsson, *The Journal of Physical Chemistry C*, 2014, **118**, 7971-7979.
- 27 K. D. Asmus, H. Moeckel and A. Henglein, *The Journal of Physical Chemistry*, 1973, **77**, 1218-1221.
- 28 D. W. Johnson and G. A. Salmon, *Journal of the Chemical Society, Faraday Transactions 1: Physical Chemistry in Condensed Phases*, 1975, **71**, 583-591.
- 29 D. Meyerstein and H. A. Schwarz, *Journal of the Chemical Society, Faraday Transactions 1: Physical Chemistry in Condensed Phases*, 1988, **84**, 2933-2949.
- 30 K. Kishore, P. N. Moorthy and K. N. Rao, *International Journal of Radiation Applications and Instrumentation*.

ARTICLE

Journal Name

- Part C. *Radiation Physics and Chemistry*, 1987, **29**, 309-313.
- 31 M. Masarwa, H. Cohen, D. Meyerstein, D. L. Hickman, A. Bakac and J. H. Espenson, *Journal of the American Chemical Society*, 1988, **110**, 4293-4297.
- 32 I. Rusonik, H. Polat, H. Cohen and D. Meyerstein, *European Journal of Inorganic Chemistry*, 2003, **2003**, 4227-4233.
- 33 P. Wardman and L. P. Candeias, *Radiation Research*, 1996, **145**, 523-531.
- 34 R. A. Sheldon and J. K. Kochi, in *Metal-catalyzed Oxidations of Organic Compounds*, ed. R. A. S. K. Kochi, Academic Press, 1981, pp. 33-70.
- 35 I. C. M. S. Santos, F. A. A. Paz, M. M. Q. Simões, M. G. P. M. S. Neves, J. A. S. Cavaleiro, J. Klinowski and A. M. V. Cavaleiro, *Applied Catalysis A: General*, 2008, **351**, 166-173.
- 36 G. R. A. Johnson, N. B. Nazhat and R. A. Saadalla-Nazhat, *Journal of the Chemical Society, Chemical Communications*, 1985, DOI: 10.1039/c39850000407, 407-408.
- 37 D. Meyerstein, *Inorganic Chemistry*, 1971, **10**, 638-641.
- 38 R. Astumian and Z. Schelly, *Journal of the American Chemical Society*, 1984, **106**, 304-308.
- 39 S. Brunauer, P. H. Emmett and E. Teller, *Journal of the American Chemical Society*, 1938, **60**, 309-319.
- 40 G. Fagerlund, *Mat. Constr.*, 1973, **6**, 239-245.
- 41 Q. Li, P. Sritharathikhun and S. Motomizu, *Analytical Sciences*, 2007, **23**, 413-417.